European Journal of Neuroscience, Vol. 11, pp. 745–752, 1999 © *European Neuroscience Association*

MINI-REVIEW
A new approach to estimate the number, density and variability of receptors at central synapses

Zoltan Nusser
Dept. of Neurology, UCLA School of Medicine, Los Angeles, CA 90095-1769, USA

Keywords: excitation, immunocytochemistry, inhibition, ion channel, neurotransmission, synapse

Introduction

Information processing within a neuronal network is influenced by the properties of synaptic connections between nerve cells. Factors that influence the behaviour of synaptic connections and the dynamics include the number of release sites between two cells, the probability of transmitter release at each site and the size of the postsynaptic response generated at each site. These parameters have traditionally been estimated with quantal analysis, a method developed and successfully applied at the neuromuscular junction (del Castillo & Katz, 1954). Miniature end-plate potentials have a Gaussian distribution with a mean value equal to the quantal size of the evoked responses. However, in most nerve cells of the central nervous system (CNS), the amplitude distributions of miniature excitatory and inhibitory postsynaptic currents (mEPSCs and mIPSCs, respectively) are not Gaussian, but are skewed towards larger values, which complicates the interpretation of quantal analysis (Jack *et al*., 1994; Walmsley, 1995). Furthermore, the size of postsynaptic responses and the transmitter release probability may not be uniform between different sites (Edwards *et al*., 1990; Korn & Faber, 1991; Jack *et al*., 1994; Dobrunz & Stevens, 1997; Markram *et al*., 1998), leaving too many unknown variables to be determined by quantal analysis alone. By combining morphological and electrophysiological analysis, the number of unknown parameters can be reduced. For example, several studies (Korn *et al*., 1982; Gulyas *et al*., 1993; Buhl *et al*., 1997) have successfully applied ultrastructural analysis to determine the number of release sites between two simultaneously recorded neurons. Furthermore, quantitative, electron microscopic autoradiography has been applied to estimate the number and density of postsynaptic nicotinic acetylcholine receptors at neuromuscular junctions (reviewed by Salpeter & Loring, 1985), however, this method has not been applied successfully at central, γ-aminobutyric acid (GABA)- or glutamatergic synapses. We have developed another combined anatomical and electrophysiological approach to estimate the size of postsynaptic responses by determining the number, density and variability of postsynaptic GABA and glutamate receptors (Nusser *et al*., 1997, 1998a, b). This method is based on electron microscopic immunogold localization of postsynaptic receptors with specific antibodies in a population of synapses (Triller *et al*., 1985; Somogyi *et al*., 1990; Baude *et al*., 1993; Phend *et al*., 1995; Matsubara *et al*., 1996), and electrophysiological estimation of the number of functional receptors present at the same population of synapses using patch-clamp recordings and non-stationary fluctuation analysis (Sigworth, 1980; Traynelis *et al*., 1993; De Koninck & Mody, 1994; Traynelis & Jaramillo, 1998). Calibrated immunogold localizations allow us to: (i) estimate the number, density and variability of functional receptors in a synapse population; (ii) compare the receptor content of distinct synapse populations; and (iii) determine changes in the synaptic receptor number following physiological or pathological alterations.

Correspondence: Z. Nusser, as above. E-mail: nusser@ucla.edu

Received 22 September 1998, revised 5 November 1998, accepted 10 November 1998

Estimating the number, density and variability of functional receptors in a synapse population

Miniature synaptic currents generated at central inhibitory synapses display a large variability in size, resulting in skewed amplitude distributions. Proposed mechanisms to account for this large variability include multiquantal transmitter release (Ropert *et al*., 1990), stochastic behaviour of channel gating (Faber *et al*., 1992), variation in the transmitter content of vesicles (Frerking *et al*., 1995), and differences in the postsynaptic receptor number at distinct sites (Edwards *et al*., 1990; Mody *et al*., 1994). We have chosen cerebellar stellate cells to investigate the mechanism underlying the variability in mIPSC amplitude, because such variability is particularly marked in these cells (Llano & Gerschenfeld, 1993); the dendritic arborization of these cells is not very extensive, allowing good voltage control of the synapses (Llano & Gerschenfeld, 1993); and these cells express only the α1, β2 and γ2 subunits of the $GABA_A$ receptor (Persohn *et al*., 1992), very likely forming a single $GABA_A$ receptor subtype with α1β2γ2 subunit composition (Angelotti & Macdonald, 1993; Tretter *et al*., 1997). Because of this restricted subunit expression in stellate cells, variability in the immunolabelling for a single subunit (e.g. α1) should reflect the variation in the total receptor number, assuming a fixed stoichiometry of $GABA_A$ receptors. In order to determine the receptor content of the entire postsynaptic area, postembedding immunogold localization was applied at the electron microscopic level on serially sectioned synapses. This method includes the rapid freezing of aldehyde-fixed brain tissue, followed by freeze-substitution with methanol at – 80 °C and embedding into acrylic resins (Lowicryl HM20, Unicryl) at – 50 °C (Baude *et al*., 1993). Serial ultrathin sections (70–90 nm thickness) were cut and reacted with specific antibodies. The antigen–antibody reactions were visualized with gold-coupled secondary antibodies, resulting in non-diffusible, particulate markers that can be quantified.

GABAergic synapses on cerebellar stellate cells showed a great variability in their α1 subunit content, some synapses contained as

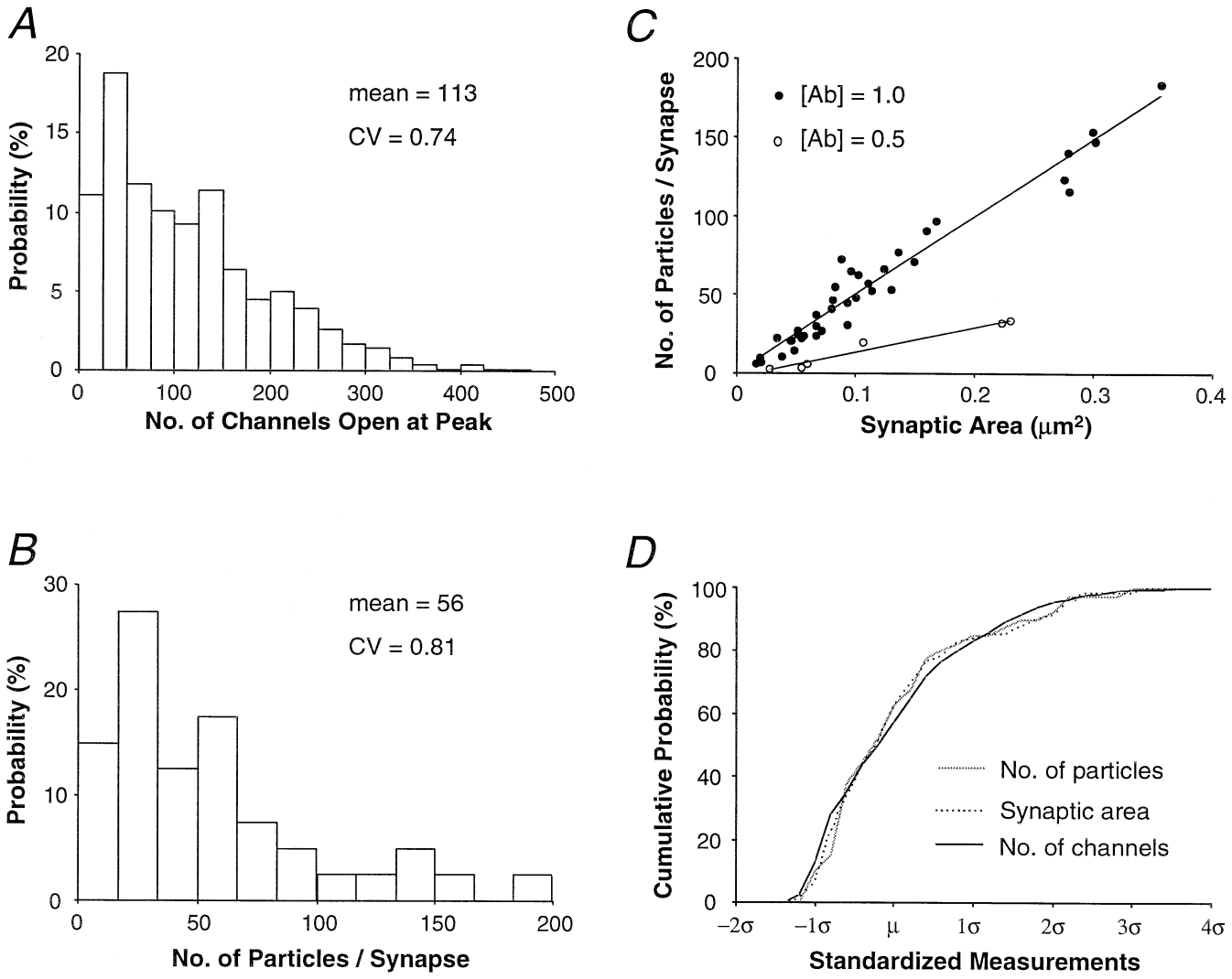

FIG. 1. Large variability in synaptic $GABA_A$ receptor number and uniform receptor density at GABAergic synapses of cerebellar stellate cells. (A,B) Comparison of the distribution of mIPSCs according to the number of channels open at their peak with the distribution of synapses according to their α1 subunit content. Both distributions are positively skewed and display a similarly large CV. The number of channels open at the peak was derived by dividing mIPSC peak amplitude, recorded in the presence of 3 μM flurazepam, by the estimated synaptic single-channel current. (C) Plot of immunoparticle number per synapse versus synaptic area for two different primary antibody concentrations ('[Ab] = 1.0', 6.3 μg protein/ml, slope of regression line = 496 particles/μm^2; '[Ab] = 0.5', 3.15 μg protein/ml, slope = 157 particles/μm^2). The positive linear correlation between immunoparticle number and synaptic area indicates a uniform receptor density across different synapses. (D) Standardized cumulative probability distributions (mean, $\mu = 0$; SD, $\sigma = 1$) of the number of channels open at the peak of the mIPSCs in flurazepam ('No. of channels'), immunoparticles per synapse ('No. of particles') and synaptic area. The distributions have similar shapes and variances, suggesting that variation in the number of receptors underlies the variability in mIPSC amplitude (adapted from Nusser *et al*., 1997).

few as six gold particles, whereas others had over 180 particles (Fig. 1B). The distribution of α1 subunits at different synapses was positively skewed with a mean of 56 gold per synapse and a coefficient of variation (CV = SD/mean) of ~0.8. This variability was the consequence of variation in the size of synaptic junctions (Fig. 1D), as a uniform receptor density was found at these GABAergic synapses (Fig. 1C).

The distribution of mIPSCs in individual stellate cells was either skewed or multimodal with a CV of ~0.7 (Llano & Gerschenfeld, 1993; Nusser *et al*., 1997). To determine how many channels underlie mIPSCs of different amplitude, peak-scaled non-stationary fluctuation analysis (Traynelis *et al*., 1993; De Koninck & Mody, 1994; Traynelis & Jaramillo, 1998) was applied. From the estimated synaptic channel conductance of 27 pS and a driving force of 80 mV, it is calculated that individual mIPSCs in stellate cells result from the opening of as few as six or as many as 380 receptors (mean ± SD = 88 ± 65). For a more direct comparison of the anatomical and physiological data, we calculated the number of channels open at the peak of mIPSCs recorded in the presence of flurazepam (a benzodiazepine agonist), because a higher receptor occupancy is expected under these conditions (Nusser *et al*., 1997). Furthermore, as the anatomical data originate from GABAergic synapses of several interneurons, mIPSCs were also pooled from several cells. The ensemble distribution of the number of channels open at the peak of the mIPSCs in flurazepam and that of the number of immunoparticles had similar shapes and variances (Fig. 1A,B,D), suggesting that variation in postsynaptic receptor number is the major determinant of mIPSC amplitude variability in these cells.

The mean number of functional receptors present at GABAergic synapses was calculated to be 140 by dividing the number of channels open at the peak of mIPSCs in flurazepam (113 channels) by the channel open probability ($P_o \approx 0.8$; Auger & Marty, 1997). To

determine the average number of functional receptors represented by a single gold particle (scaling factor), the functional receptor number (140) was divided by the mean number of immunoparticles per synapse (56), providing a scaling factor of 2.5. The relatively high receptor labelling efficiency (~ 40%) may result from the fact that each $GABA_A$ receptor contains two α-subunits (Tretter *et al*., 1997) and, as polyclonal antibodies were used, on each subunit more than one epitope may be recognized. Thus, the epitope labelling efficiency may not be more than 10%. Similarly, the relatively high labelling efficiency for α-amino-3-hydroxy-5-methyl-4-isoxazolepropionate (AMPA) receptors (~ 45%, see below) may require the labelling of no more than 5% of the epitopes (given a tetrameric structure of the receptors and several epitopes per subunit). The 5–10% epitope labelling efficiency is consistent with the fact that under postembedding conditions, only epitopes close to the surface (within ~ 6 nm; Kellenberger *et al*., 1987) of the ultrathin section are recognized by the antibodies. The scaling factor, of course, depends on the primary and secondary antibodies and on other technical factors, e.g. the fixation condition and type of resin employed. Nevertheless, the density of synaptic $GABA_A$ receptors in stellate cells can be calculated by multiplying the immunoparticle density (~ 500 particles/μm^2) by the scaling factor (2.5), resulting in an estimated 1250 receptors/μm^2. Interestingly, $GABA_A$ receptor density was also found to be uniform at GABAergic synapses on cerebellar Purkinje cells (Somogyi *et al*., 1998), as well as on hippocampal granule cells (Nusser *et al*., 1998a). However, the receptor density is not constant across cell types. Moreover, even two different compartments of a single cell type, e.g. the soma versus axon initial segment (500 versus 850 receptors/μm^2, respectively) of hippocampal granule cells, can have different receptor densities. These density values are an order of magnitude lower than those obtained for the nicotinic acetylcholine receptors at the neuromuscular junction (more than 8000 receptors/μm^2; Fertuck & Salpeter, 1974). Thus, $GABA_A$ receptor packing density is not maximal, supporting the view that postsynaptic receptors are arranged in small 'microclusters' which are separated by receptor-free spaces (Mody *et al*., 1994; Nusser *et al*., 1997). Indeed, immunoparticles are not evenly distributed within a synaptic junction, but the clustering of particles was observed in GABAergic synapses of cerebellar stellate cells (Nusser *et al*., 1997), Purkinje cells (Somogyi *et al*., 1996), as well as hippocampal granule cells (Nusser *et al*., 1998a).

Comparing the receptor content of distinct synapse populations

It may not be possible to obtain a reliable estimate of the size of postsynaptic responses at certain synapses using physiological approaches alone, because of technical limitations, e.g. the inaccessibility of the synapse with recording pipettes, unknown amount of alterations due to electrotonic filtering by the dendritic tree or improper voltage clamp. For example, estimates of quantal size at spine synapses on hippocampal pyramidal cells vary over a large range. Some studies indicated the presence of over 150 AMPA/kainate receptors (Jack *et al*., 1994; Forti *et al*., 1997), others suggested either a very low receptor number (Stevens & Wang, 1994; Bolshakov & Siegelbaum, 1995) or even the presence of synapses without any AMPA/kainate receptors (reviewed by Malenka & Nicoll, 1997). In contrast, there is a thorough analysis concerning the number of functional AMPA/kainate receptors at hippocampal mossy fibre to CA3 pyramidal cell synapses (Jonas *et al*., 1993). The mEPSCs of mossy fibre origin in 15–24-day-old rats (P15–P24) have an average peak conductance of 418 pS. Given a single channel conductance of 8.5 pS, a maximum P_o of 0.71 and a receptor occupancy of 0.85

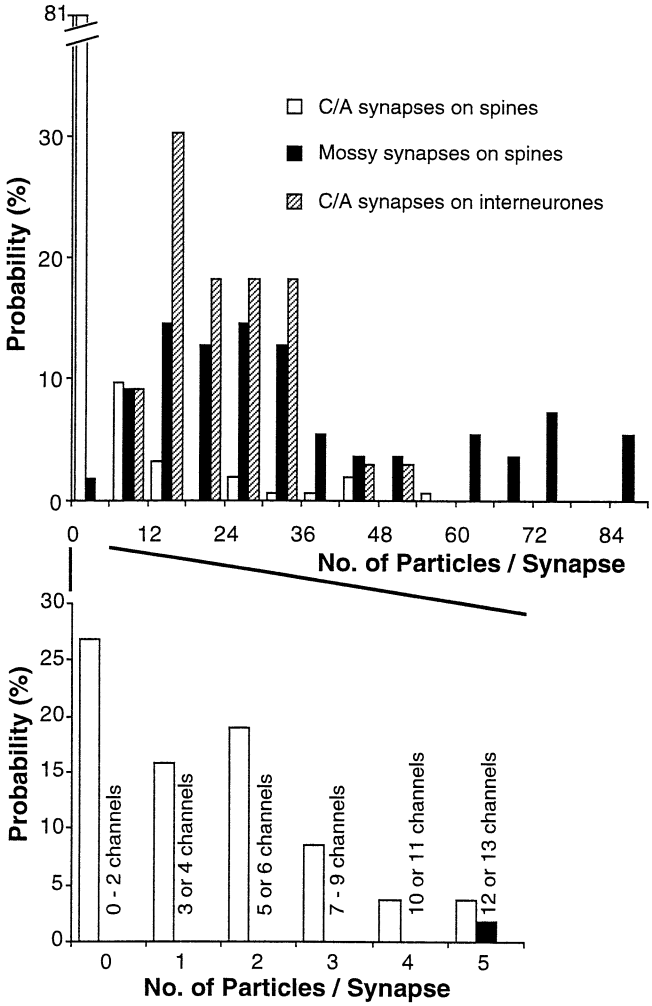

FIG. 2. Distinct patterns in the AMPA receptor content of functionally different glutamatergic synapses in the CA3 area of the rat hippocampus (17 day old). Synapses made by C/A terminals on pyramidal cell spines (open columns) have a positively skewed distribution (4.6 ± 9.2, mean ± SD) with ~ 28% of them being immunonegative. In the stratum radiatum, C/A synapses on GABAergic interneurons (striped columns) contain 22.2 ± 10.4 particles and have a Gaussian distribution. No immunonegative asymmetrical synapse is found on interneuron dendrites. Mossy synapses (black columns) on complex spines of pyramidal cells are all immunopositive, and have a skewed distribution with a mean number of particles per synapse of 35.3 ± 23.3. The bottom panel shows the re-binned data of the first bin of the distribution (indicated by the thick lines) and the corresponding number of functional AMPA receptors calculated after calibration (1 gold = 2.3 channels; adapted from Nusser *et al*., 1998b).

(Jonas *et al*., 1993), on average 81 functional AMPA/kainate receptors are estimated to be present at mossy synapses (for calculation see Jonas *et al*., 1993; Nusser *et al*., 1998b). We used this number to calibrate the immunosignal for the AMPA-type glutamate receptors (GluRs) at mossy synapses and applied this calibration to other glutamatergic synapses to estimate their AMPA receptor content.

Serial ultrathin sections of the hippocampus of P17 rats were immunoreacted for all AMPA-type GluR subunits (GluR1–4) with a mixture of antibodies against GluR2/3 and GluR1–4 subunits, and every synapse between mossy fibre terminals and pyramidal cell complex spines was analysed within the sampled volume of tissue (Nusser *et al*., 1998b). All mossy fibre synapses were immunopositive, and the number of gold particles formed a non-Gaussian, skewed distribution (Fig. 2) with a CV of ~ 0.65. Synaptic areas had a very

similar distribution and variance, reflecting a uniform AMPA receptor density (~ 500 receptors/μm^2) across mossy synapses. The average number of 35 gold particles per mossy synapse provided a scaling factor of ~ 2.3 (= 81/35).

In addition to mossy fibre terminals in the stratum lucidum, pyramidal cells in the CA3 area also receive glutamatergic input from commissural and associational (C/A) terminals in the strata radiatum and oriens, and from entorhinal fibres in the stratum laconosum-moleculare. This multiple glutamatergic innervation of this cell type allowed us to investigate the extent to which the pattern of AMPA receptor expression is influenced by the presynaptic input. Synapses made by C/A terminals in the stratum radiatum showed a large variability in their receptor content, some contained over 60 gold particles, whereas others were immunonegative (Fig. 3). The distribution of AMPA receptor content at these synapses was skewed (Fig. 2; mean = 4.6, CV = 2.0) with ~ 28% of them being immunonegative. These results predict that 28% of the C/A synapses on P17 pyramidal spines contain less than three functional receptors, whereas the largest synapses have more than 120 receptors (mean ≈ 11). A very similar pattern of receptor labelling was observed at spine synapses in the stratum radiatum of the CA1 and CA3 areas of adult rats, but a smaller proportion of synapses was immunonegative in adult animals compared to juvenile rats (15% versus 28%, respectively). The variability in synaptic area could not account for the variation in the synaptic receptor number, indicating that synaptic receptor density is also variable on spine synapses. Indeed, a much larger variability in receptor density was found at small than large synapses (figure 4 in Nusser *et al*., 1998b). Hence, characteristic differences between the distribution of AMPA receptors at mossy versus C/A synapses include the lack of immunonegative synapses, on average four–eight times higher number of gold particles per synapse, and a much smaller variability in the receptor content of mossy synapses. These results demonstrate that the number of postsynaptic AMPA receptors cannot be determined by the postsynaptic cell alone.

In order to test the influence of the postsynaptic cell on receptor expression, we compared the AMPA receptor content of synapses on distinct cell types innervated by a common afferent. The cell bodies and dendrites of GABAergic interneurons are distributed throughout the hippocampal layers and receive synaptic inputs from C/A fibres, which also innervate pyramidal cell spines. Every asymmetrical synapse on dendritic shafts of interneurons was strongly immunopositive for AMPA receptors (Fig. 2). As a consequence of the consistent, strong labelling and the lack of immunonegative synapses, these synapses contained, on average, five times as many gold particles as C/A synapses on pyramidal cell spines. The distribution of AMPA receptors at interneuron synapses was Gaussian with a CV of < 0.5. Thus, we predict the presence of ~ 50 ± 25 (range: 16–110) functional AMPA receptors at glutamatergic synapses of GABAergic interneurons. As the quantitative pattern of AMPA receptor expression is very different in two cell types innervated by a common afferent, it is concluded that the amount of AMPA receptor at a given glutamatergic synapse is governed by both pre- and postsynaptic elements.

The very skewed distribution of gold particles at spine synapses in the stratum radiatum belonging to pyramidal cells indicates that these synapses do not form a homogeneous population with regard to their AMPA receptor content. In adult rats, ~ 15% of the synapses have less than three functional AMPA receptors (assuming a similar scaling factor in adult and P17 rats), the majority of the synapses (~ 65%) contain between three and 23 receptors, and ~ 20% of the spine synapses accommodate a large number of AMPA receptors (25–200). These results may provide an explanation for the wide range in estimates of postsynaptic receptor number at hippocampal spine synapses (Jack *et al*., 1994; Stevens & Wang, 1994; Bolshakov & Siegelbaum, 1995; Forti *et al*., 1997). Furthermore, it is likely that the distribution recorded at any one time is just a snapshot of a dynamically changing pattern. Cellular events may convert AMPA receptor negative synapses into weakly positive ones and eventually strongly positive ones (reviewed by Ben-Ari *et al*., 1997; Malenka & Nicoll, 1997). This process may require action potentials in the postsynaptic cell to occur consistently shortly after the presynaptic release of transmitter (Markram *et al*., 1997; Debanne *et al*., 1998; Zhang *et al*., 1998). However, if the activities of pre- and postsynaptic neurons are not correlated, or action potential firing of the postsynaptic cell consistently precedes the presynaptic action potential, a reverse process may reduce the number of synaptic AMPA receptors and may eventually eliminate the connection.

Our results, showing that a significant proportion of Schaffer collateral and C/A synapses on pyramidal cell spines have very few (< three) if any functional AMPA receptors, are in agreement with the suggestion that some glutamatergic synapses of the hippocampus and neocortex do not contain functional AMPA receptors (reviewed by Malenka & Nicoll, 1997). The presence of so-called 'silent' glutamatergic synapses in the hippocampus has been proposed by several studies on the basis of *in vitro* electrophysiological experiments showing that, at hyperpolarized potentials, no fast postsynaptic response could be detected, although from the same stimulus site when the postsynaptic neuron was depolarized, *N*-methyl-D-aspartate (NMDA) receptor-mediated postsynaptic responses could be observed (reviewed by Malenka & Nicoll, 1997). It has also been proposed that the transformation of synapses containing only NMDA receptors into AMPA/NMDA receptor-containing ones may underlie the expression of NMDA receptor-dependent long-term potentiation (LTP, reviewed by Malenka & Nicoll, 1997) and functional synapse formation during postnatal development (reviewed by Ben-Ari *et al*., 1997). The finding that the proportion of immunonegative spine synapses in the stratum radiatum of a P17 rat is almost twice as high as that in adult rats is in line with these suggestions.

Mossy fibre and C/A synapses on CA3 pyramidal cells have different functional properties, and our results reveal differences in their AMPA receptor content. Interestingly, these two connections exhibit different forms of synaptic plasticity. The induction of LTP at C/A synapses requires the activation of the NMDA-type GluRs, whereas LTP at mossy fibre synapses is independent of NMDA receptor activation (Nicoll & Malenka, 1995). Schaffer collateral synapses on CA1 pyramidal cell spines also exhibit NMDA receptor-dependent LTP and show a similar pattern of AMPA receptor expression to the C/A spine synapses, with a significant proportion of synapses having no or very few receptors. Such similar characteristics suggest that this pattern of AMPA receptor content may be a general feature of glutamatergic synapses that display NMDA receptor-

FIG. 3. C/A synapses on pyramidal cell spines in the hippocampal CA3 area show a large variability in their AMPA receptor content. (A_1–A_3) Serial ultrathin sections of the stratum radiatum demonstrate that some synapses (arrows) made by C/A terminals (b) with pyramidal cell spines (s_1 and s_2) contain a large number of gold particles, whereas other asymmetrical synapses (open arrows) on spines (s^-) are immunonegative (ab-pan-AMPA + ab-GluR2/3). A bouton (b_2) makes two release sites with two spines (s^- and s_2), one of which (open arrow) is immunonegative and is fully shown. The other one (arrow) was present in five serial sections (two are shown) and contained 31 gold particles. Some particles are also present on extrasynaptic spine membranes (small arrows). Scale bar: 0.2 μm (adapted from Nusser *et al*., 1998b).

dependent LTP. This is supported by the finding that GABAergic interneurons which generally do not show NMDA receptor-dependent LTP (for review see McBain *et al*., 1999) exhibit an AMPA receptor content very different from Schaffer collateral and C/A synapses, but more similar to that of mossy fibre synapses. The identification of distinct molecular fingerprints for these different types of connection

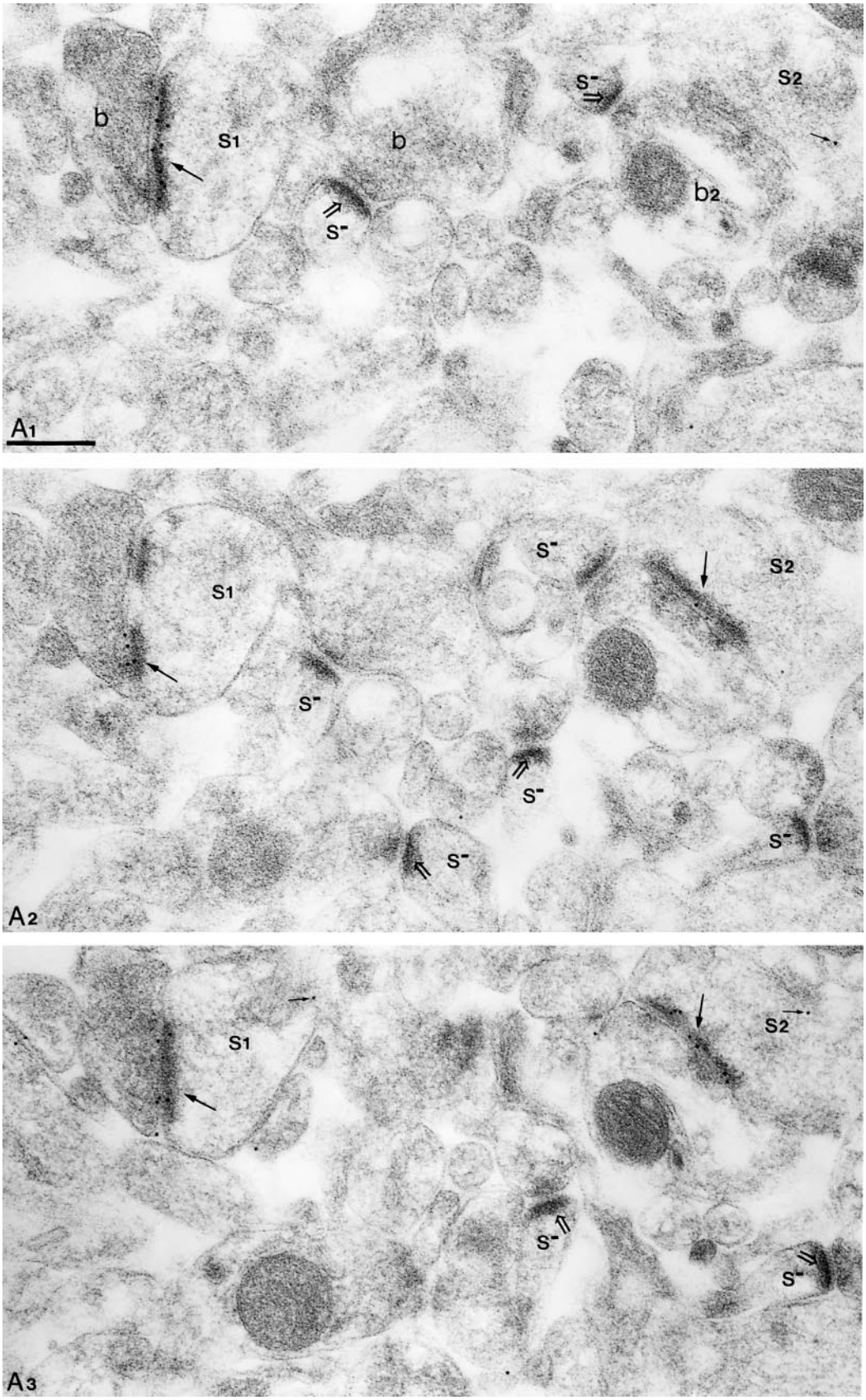

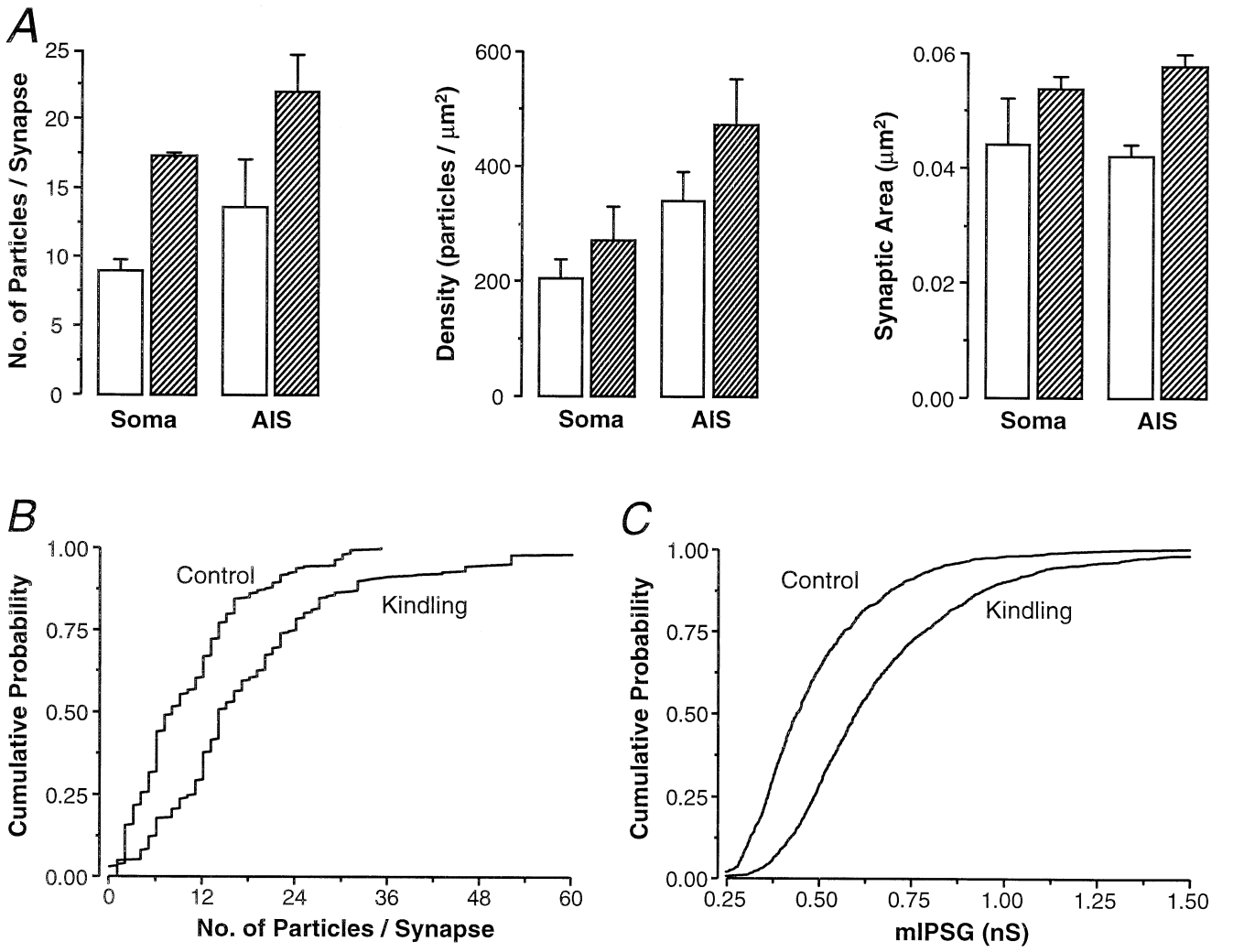

FIG. 4. Increase in the number of synaptic $GABA_A$ receptors underlies the augmented GABAergic inhibition in kindled hippocampal granule cells. (A) The mean number of immunoparticles for the β2/3 subunits of the $GABA_A$ receptor at perisomatic inhibitory synapses on granule cells was significantly larger in kindled (striped columns) than control (open columns) rats. This enhancement was the consequence of an increased immunoparticle density as well as an enlargement in the area of somatic and AIS synapses (mean ± SD are indicated, $n = 3$ animals each). (B) Cumulative weighted distributions of immunoparticles at AIS and somatic synapses in control and kindled preparations (pooled from three animals each). (C) Distributions of mIPSC conductance (mIPSG) recorded in control and kindled granule cells (pooled from four cells each; adapted from Nusser *et al*., 1998a).

will help us to predict the functional properties and type of plasticity of other excitatory connections of the brain.

Determining changes in synaptic receptor number following physiological or pathological alterations

Another promising feature of the calibrated immunogold localization is that it can be used to reveal changes in the receptor content of synapses upon physiological and pathological alterations. Therefore, we applied this method to investigate the relationship between the number of postsynaptic $GABA_A$ receptors and quantal size (q) following long-term GABAergic synaptic plasticity (Otis *et al*., 1994) induced by an experimental model of temporal lobe epilepsy (kindling, McNamara, 1994). Quantal analysis (Edwards *et al*., 1990) of minimal stimulus-evoked IPSCs in control hippocampal granule cells revealed an average q of 435 pS, which increased to 722 pS after kindling (Nusser *et al*., 1998a). This increase in q was not the consequence of an augmented single-channel conductance, as peak-scaled non-stationary variance analysis yielded similar mean conductances in control (20.6 pS) and kindled (21.3 pS) granule cells. Considering full occupancy of postsynaptic $GABA_A$ receptors (Edwards *et al*., 1990; De Koninck & Mody, 1994) and a maximum P_o of 0.8 (Auger & Marty, 1997), on average 26 (= 435 pS/[21 pS × 0.8]) functional receptors are calculated to be present at perisomatic GABAergic synapses of control granule cells. An almost identical estimate of the postsynaptic receptor number was obtained from the median value of the mIPSC distribution (436 pS).

Quantitative immunogold localization of the β2 and β3 (β2/3) subunits of the $GABA_A$ receptor in perisomatic inhibitory synapses revealed an increase in the immunoreactive receptor content of both somatic (94% increase) and axon initial segment (AIS, 61% increase) synapses after kindling. This increase was the consequence of an enlarged synaptic area and an augmented receptor density (Fig. 4A). The weighted distribution of somatic and AIS synapses of control granule cells (includes 64% somatic and 36% AIS synapses to reflect their natural occurrence on granule cells; Kosaka, 1996) with regard to their β2/3 subunit content was positively skewed (Fig. 4B) with a mean of 10.2 particles per synapse, resulting in a scaling factor of ~ 2.5 (= 26/10.2). The large variability (CV in control: 0.76; CV in kindling: 0.74) and the skewed distribution persisted after kindling

with an approximately parallel shift (~ 75% increase) in the cumulative probability plot (Fig. 4B). A similar shift was observed in the cumulative distribution of mIPSC conductances (Fig. 4C), with a smaller increase in the median value (41%). This discrepancy in the increase in receptor number versus mIPSC amplitude may be due to changes in some non-overlapping population of synapses sampled for mIPSCs and anatomical analysis. In contrast to miniature currents, there was a good match between the increase in quantal size of the evoked responses and immunolabelled receptors. These findings demonstrate the postsynaptic insertion of new $GABA_A$ receptors and the corresponding increase in postsynaptic responses as the mechanism of augmenting efficacy at inhibitory synapses **(**see also Wan *et al*., 1997).

The direct measurements of q and the immunolabelled receptor number in control and kindled animals enabled us to demonstrate an alteration in P_o. As the mean number of particles increased to 18.5 after kindling with a scaling factor of 2.5, an average of 47 $GABA_A$ receptors is calculated to be present at kindled synapses. From q (722 pS) and the channel conductance (21.3 pS) after kindling, an average of 34 $GABA_A$ receptors is calculated to open at the peak of synaptic currents. Thus, an average P_o of 0.72 (= 34/47) is predicted at kindled GABAergic synapses. It is important to note that the decrease in P_o is independent of the initial estimate of P_o at control synapses. It is likely that the reduction in P_o does not take place at every synapse, only at some large synapses where the synaptic area and receptor number exceed a certain limit. It has been reported (Nusser *et al*., 1997) that for cerebellar stellate cells, postsynaptic $GABA_A$ receptors are fully occupied at synapses containing less than ~ 80 receptors (corresponding to 33 particles in dentate granule cells). Our finding, that 99% of the perisomatic synapses in control granule cells contain < 33 particles, is in line with the predicted full receptor occupancy at most of these synapses (Edwards *et al*., 1990; De Koninck & Mody, 1994). However, more than 10% of the kindled synapses contained > 33 particles, consistent with an incomplete occupancy of the receptors. There are two important consequences of this change in the operation of large synapses following kindling-induced plasticity. First, further insertion of receptors into the postsynaptic membrane will no longer linearly increase postsynaptic responses. Thus, more effective ways of further facilitation include the increase of the probability of transmitter release or the generation of new synapses. Second, the size of the IPSCs will also depend on presynaptic factors, e.g. the transmitter concentration in the cleft, and its fluctuation will be reflected in the postsynaptic responses.

Conclusions

We have developed a novel approach, combining high-resolution quantitative immunogold localization of synaptic receptors and patch-clamp recordings of postsynaptic responses, to investigate synaptic transmission in the CNS. This method allowed us to identify the large variability in the postsynaptic $GABA_A$ receptor number, resulting in highly variable postsynaptic responses. We also found that the number, density and variability in synaptic AMPA-type GluRs are determined by both pre- and postsynaptic factors in a way that functionally distinct glutamatergic connections display characteristic patterns of receptor expression. This approach has also been used to establish the synaptic insertion of $GABA_A$ receptors and the corresponding increase in postsynaptic responses augmenting the efficacy at inhibitory synapses. The development of new ways of calibration (e.g. using standard series with different amounts of antigene; Ottersen, 1989) will further boost the application of high-resolution, quantitative immunogold methods to study the role of strategically placed proteins in synaptic communications.

Acknowledgements

I would like to thank Drs Mark Farrant, Istvan Mody and Peter Somogyi for their comments on the manuscript. Z.N. is supported by a Wellcome Prize Travelling Research Fellowship.

Abbreviations

AIS, axon initial segment; AMPA, α-amino-3-hydroxy-5-methyl-4-isoxazolepropionate; C/A, commissural and associational; CNS, central nervous system; CV, coefficient of variation; GABA, γ-aminobutyric acid; GluR, glutamate receptor; LTP, long-term potentiation; mEPSCs, miniature excitatory postsynaptic currents; mIPSCs, miniature inhibitory postsynaptic currents; NMDA, *N*-methyl-D-aspartate; P_o, channel open probability; q, quantal size.

References

Angelotti, T.P. & Macdonald, R.L. (1993) Assembly of $GABA_A$ receptor subunits: α1β1 and α1β1γ2s subunits produce unique ion channels with dissimilar single-channel properties. *J. Neuroscience*, **13**, 1429–1440.

Auger, C. & Marty, A. (1997) Heterogeneity of functional synaptic parameters among single release sites. *Neuron*, **19**, 139–150.

Baude, A., Nusser, Z., Roberts, J.D.B., Mulvihill, E., McIlhinney, R.A. & Somogyi, P. (1993) The metabotropic glutamate receptor (mGluR1α) is concentrated at perisynaptic membrane of neuronal subpopulations as detected by immunogold reaction. *Neuron*, **11**, 771–787.

Ben-Ari, Y., Khazipov, R., Leinekugel, X., Caillard, O. & Gaiarsa, J.L. (1997) $GABA_A$, NMDA and AMPA receptors: a developmentally regulated 'menage a trois'. *Trends Neurosci.*, **20**, 523–529.

Bolshakov, V.Y. & Siegelbaum, S.A. (1995) Regulation of hippocampal transmitter release during development and long-term potentiation. *Science*, **269**, 1730–1734.

Buhl, E.H., Tamas, G., Szilagyi, T., Stricker, C., Paulsen, O. & Somogyi, P. (1997) Effect, number and location of synapses made by single pyramidal cells onto aspiny interneurones of cat visual cortex. *J. Physiol.* (*Lond.*), **500**, 689–713.

Debanne, D., Gahwiler, B.H. & Thompson, S.M. (1998) Long-term synaptic plasticity between pairs of individual CA3 pyramidal cells in rat hippocampal slice cultures. *J. Physiol.* (*Lond.*), **507**, 237–247.

De Koninck, Y. & Mody, I. (1994) Noise analysis of miniature IPSCs in adult rat brain slices: properties and modulation of synaptic $GABA_A$ receptor channels. *J. Neurophysiol.*, **71**, 1318–1335.

del Castillo, J. & Katz, B. (1954) Quantal components of the end-plate potential. *J. Physiol.* (*Lond.*), **124**, 560–573.

Dobrunz, L.E. & Stevens, C.F. (1997) Heterogeneity of release probability, facilitation, and depletion at central synapses. *Neuron*, **18**, 995–1008.

Edwards, F.A., Konnerth, A. & Sakmann, B. (1990) Quantal analysis of inhibitory synaptic transmission in the dentate gyrus of rat hippocampal slices: a patch-clamp study. *J. Physiol.* (*Lond.*), **430**, 213–249.

Faber, D.S., Young, W.S., Legendre, P. & Korn, H. (1992) Intrinsic quantal variability of receptor-transmitter interactions. *Science*, **258**, 1494–1498.

Fertuck, H.C. & Salpeter, M.M. (1974) Localization of acetylcholine receptor by ^{125}I-labeled α bungarotoxin binding at mouse motor endplates. *Proc. Natl. Acad. Sci. USA*, **71**, 1376–1378.

Forti, L., Bossi, M., Bergamaschi, A., Villa, A. & Malgaroli, A. (1997) Loose-patch recordings of single quanta at individual hippocampal synapses. *Nature*, **388**, 874–878.

Frerking, M., Borges, S. & Wilson, M. (1995) Variation in GABA mini amplitude is the consequence of variation in transmitter concentration. *Neuron*, **15**, 885–895.

Gulyas, A.I., Miles, R., Sik, A., Toth, K., Tamamaki, N. & Freund, T.F. (1993) Hippocampal pyramidal cells excite inhibitory neurons through a single release site. *Nature*, **366**, 683–687.

Jack, J.J.B., Larkman, A.U., Major, G. & Stratford, K.J. (1994) Quantal analysis of the synaptic excitation of CA1 hippocampal pyramidal cells. In Stjarne, L., Greengard, P., Grillner, S., Hokfelt, T. & Ottoson, D. (eds), *Molecular and Cellular Mechanisms of Neurotransmitter Release*. Raven Press, New York, pp. 275–299.

Jonas, P., Major, G. & Sakmann, B. (1993) Quantal components of unitary

EPSCs at the mossy fibre synapse on CA3 pyramidal cells of rat hippocampus. *J. Physiol.* (*Lond.*), **472**, 615–663.
Kellenberger, E., Durrenberger, M., Villiger, W., Carlemalm, E. & Wurtz, M. (1987) The efficiency of immunolabel on Lowicryl sections compared to theoretical predictions. *J. Histochem. Cytochem.*, **35**, 959–969.
Korn, H. & Faber, D.S. (1991) Quantal analysis and synaptic efficacy in the CNS. *Trends Neurosci.*, **14**, 439–445.
Korn, H., Mallet, A., Triller, A. & Faber, D.S. (1982) Transmission at a central inhibitory synapse. II. Quantal description of release, with a physical correlate for binomial *n*. *J. Neurophysiol.*, **48**, 679–707.
Kosaka, T. (1996) Synapses in the granule cell layer of the rat dentate gyrus: serial-sectioning study. *Exp. Brain Res.*, **112**, 237–243.
Llano, I. & Gerschenfeld, H.M. (1993) Inhibitory synaptic currents in stellate cells of rat cerebellar slices. *J. Physiol.* (*Lond.*), **468**, 177–200.
Malenka, R.C. & Nicoll, R.A. (1997) Silent synapses speak up. *Neuron*, **19**, 473–476.
Markram, H., Lubke, J., Frotscher, M. & Sakmann, B. (1997) Regulation of synaptic efficacy by coincidence of postsynaptic APs and EPSPs. *Science*, **275**, 213–215.
Markram, H., Wang, Y. & Tsodyks, M. (1998) Differential signaling via the same axon of neocortical pyramidal neurons. *Proc. Natl. Acad. Sci. USA*, **95**, 5323–5328.
Matsubara, A., Laake, J.H., Davanger, S., Usami, S. & Ottersen, O.P. (1996) Organization of AMPA receptor subunits at a glutamate synapse: a quantitative immunogold analysis of hair cell synapses in the rat organ of Corti. *J. Neuroscience*, **16**, 4457–4467.
McBain, C.J., Freund, T.F. & Mody, I. (1999) Glutamatergic synapses onto hippocampal interneurones: precision timing without lasting plasticity. *Trends Neurosci.* (in press).
McNamara, J.O. (1994) Cellular and molecular basis of epilepsy. *J. Neuroscience*, **14**, 3413–3425.
Mody, I., De Koninck, Y., Otis, T.S. & Soltesz, I. (1994) Bridging the cleft at GABA synapses in the brain. *Trends Neurosci.*, **17**, 517–525.
Nicoll, R.A. & Malenka, R.C. (1995) Contrasting properties of two forms of long-term potentiation in the hippocampus. *Nature*, **377,** 115–118.
Nusser, Z., Cull-Candy, S.G. & Farrant, M. (1997) Differences in synaptic $GABA_A$ receptor number underlie variation in GABA mini amplitude. *Neuron*, **19**, 697–709.
Nusser, Z., Hajos, N., Somogyi, P. & Mody, I. (1998a) Increased number of synaptic $GABA_A$ receptors underlies potentiation at hippocampal inhibitory synapses. *Nature*, **395**, 172–177.
Nusser, Z., Lujan, R., Laube, G., Roberts, J.D.B., Molnar, E. & Somogyi, P. (1998b) Cell type and pathway dependence of synaptic AMPA receptor number and variability in the hippocampus. *Neuron*, **21**, 545–559.
Otis, T.S., De Korninck, Y. & Mody, I. (1994) Lasting potentiation of inhibition is associated with an increased number of γ-aminobutyric acid type A receptors activated during miniature inhibitory postsynaptic currents. *Proc. Natl. Acad. Sci. USA*, **91**, 7698–7702.
Ottersen, O.P. (1989) Quantitative electron microscopic immunocytochemistry of neuroactive amino acids. *Anat. Embryol.*, **180**, 1–15.
Persohn, E., Malherbe, P. & Richards, J.G. (1992) Comparative molecular neuroanatomy of cloned $GABA_A$ receptor subunits in the rat CNS. *J. Comp. Neurol.*, **326**, 193–216.
Phend, K.D., Rustioni, A. & Weinberg, R.J. (1995) An osmium-free method of Epon embedment that preserves both ultrastructure and antigenicity for post-embedding immunocytochemistry. *J. Histochem. Cytochem.*, **43**, 283–292.
Ropert, N., Miles, R. & Korn, H. (1990) Characteristics of miniature inhibitory postsynaptic currents in CA1 pyramidal neurones of rat hippocampus. *J. Physiol.* (*Lond.*), **428**, 707–722.
Salpeter, M.M. & Loring, R.H. (1985) Nicotinic acetylcholine receptors in vertebrate muscle: properties, distribution and neural control. *Prog. Neurobiol.*, **25**, 297–325.
Sigworth, F.J. (1980) The variance of sodium current fluctuations at the node of Ranvier. *J. Physiol.* (*Lond.*), **307**, 97–129.
Somogyi, P., Eshhar, N., Teichberg, V.I. & Roberts, J.D.B. (1990) Subcellular localization of a putative kainate receptor in bergmann glial cells using a monoclonal antibody in the chick and fish cerebellar cortex. *Neuroscience*, **35**, 9–30.
Somogyi, P., Fritschy, J.-M., Benke, D., Roberts, J.D.B. & Sieghart, W. (1996) The γ2 subunit of the $GABA_A$ receptor is concentrated in synaptic junctions containing the α1 and β2/3 subunits in hippocampus, cerebellum and globus pallidus. *Neuropharmacology*, **35**, 1425–1444.
Somogyi, P., Nusser, Z., Roberts, J.D.B. & Lujan, R. (1998) Precision and variability in the placement of pre- and postsynaptic receptors in relation to neurotransmitter release sites. In Faber, D.S., Korn, H., Thompson, S.M., Redman, S.F. & Altman, F.S. (eds), *Central Synapses: Quantal Mechanisms and Plasticity.* HFSP, Strasbourg, Vol. 4, pp. 82–93.
Stevens, C.F. & Wang, Y. (1994) Changes in reliability of synaptic function as a mechanism for plasticity. *Nature*, **371**, 704–707.
Traynelis, S.F., Silver, R.A. & Cull-Candy, S.G. (1993) Estimated conductance of glutamate receptor channels activated during EPSCs at the cerebellar mossy fiber-granule cell synapses. *Neuron*, **11**, 279–289.
Traynelis, S.F. & Jaramillo, F. (1998) Getting the most out of noise in the central nervous system. *Trends Neurosci.*, **21**, 137–145.
Tretter, V., Ehya, N., Fuchs, K. & Sieghart, W. (1997) Stoichiometry and assembly of a recombinant $GABA_A$ receptor subtype. *J. Neuroscience*, **17**, 2728–2737.
Triller, A., Cluzeaud, F., Pfeiffer, F., Betz, H. & Korn, H. (1985) Distribution of glycine receptors at central synapses: an immunoelectron microscopy study. *J. Cell. Biol.*, **101**, 683–688.
Walmsley, B. (1995) Interpretation of 'quantal' peaks in distributions of evoked synaptic transmission at central synapses. *Proc. R. Soc. Lond. B*, **261**, 245–250.
Wan, Q., Xiong, Z.G., Man, H.Y., Ackerley, C.A., Braunton, J., Lu, W.Y., Becker, L.E., MacDonald, J.F. & Wang, Y.T. (1997) Recruitment of functional $GABA_A$ receptors to postsynaptic domains by insulin. *Nature*, **388**, 686–690.
Zhang, L.I., Tao, H.-W., Holt, C.E., Harris, W.A. & Poo, M. (1998) A critical window for cooperation and competition among developing retinotectal synapses. *Nature*, **395**, 37–44.